DALTON
FULL PAPER

High yield synthesis of Ru–Pt mixed-metal cluster compounds

Sophie Hermans, Tetyana Khimyak and Brian F. G. Johnson*

University Chemical Laboratories, Lensfield Road, Cambridge, UK CB2 1EW

Received 3rd July 2001, Accepted 11th September 2001
First published as an Advance Article on the web 23rd October 2001

The reaction of $[PPN]_2[Ru_5C(CO)_{14}]$ **1** or $[PPN]_2[Ru_6C(CO)_{16}]$ **2** [$PPN^+ = (PPh_3)_2N^+$] with Pt(II) compounds of general formula $[PtX_2Cl_2]$ [X_2 = (COD), $(PPh_3)_2$ and $(PPh_3)(CO)$] (COD = 1,5-cyclooctadiene) have been investigated and the products of simple or double addition, *viz*. $[Ru_5PtC(CO)_{14}(COD)]$ **3**, $[Ru_5PtC(CO)_{14}(PPh_3)_2]$ **4**, $[Ru_5PtC(CO)_{15}(PPh_3)]$ **5**, $[Ru_5Pt_2C(CO)_{15}(PPh_3)_2]$ **6**, $[Ru_6PtC(CO)_{16}(COD)]$ **7**, $[Ru_6Pt_2C(CO)_{15}(COD)_2]$ **8**, obtained. The molecular and crystal structures of **3**–**8** have been established by single crystal X-ray analysis. Compounds **3**–**7** all contain an intact Ru core with Pt fragment(s) capping triangular or square faces. The resulting mixed-metal core is octahedral for the clusters Ru_5Pt and face-capped octahedral for the clusters Ru_nPt_m (n = 5 or 6; m = 2 or 1). Only compound **8** did not follow this pattern, with the Pt fragments bridging two Ru–Ru edges of the otherwise unaltered Ru_6C core.

Introduction

Mixed-metal clusters have been shown to be ideal precursors for the preparation of supported bimetallic nanoparticles of well-defined sizes and composition.[1–3] Such nanoparticles have been shown to be firmly anchored onto the siliceous support and highly active for catalytic hydrogenations under solvent-free and mild temperature conditions. Moreover, we have demonstrated that their selectivity may be tuned by varying the nature of the two metals in the cluster precursor.[2] As a consequence of these observations, we have directed our efforts toward the synthesis of high nuclearity clusters in high yield. Herein we report the synthesis and characterisation of a series of Ru–Pt mixed-metal clusters with Ru : Pt ratios of 5 : 1, 5 : 2, 6 : 1 or 6 : 2. All were obtained following a common synthetic strategy, starting from dianionic ruthenium clusters, in reactions with di-chloro mononuclear complexes of Pt(II) in the presence of silica. The silica acts as an effective chloride scavenger, to produce *in situ* dicationic platinum fragments which appear to be stabilised by a direct interaction with the silica surface. This approach has led to highly predictable products in high yields.

Results and discussion

The salt $[PPN]_2[Ru_5C(CO)_{14}]$ **1** was reacted with one equivalent of $[Pt(COD)Cl_2]$ in dichloromethane at room temperature in the presence of silica. The expected compound $[Ru_5PtC(CO)_{14}(COD)]$ **3** was the only product of the reaction, and could be isolated in 84% yield as a red microcrystalline powder. In the infrared spectrum peaks corresponding to terminal and bridging carbonyl ligands were observed. In its mass spectrum a molecular peak was observed at *m*/*z* 1214, followed by peaks corresponding to fragments generated by the loss of the COD ligand. This, in turn, was followed by 14 peaks corresponding to the sequential loss of CO ligands, leading to a peak at *m*/*z* 713 attributable to the bare Ru_5PtC core. The ^{13}C NMR spectrum in $CDCl_3$ displayed a peak at 87.37 ppm and at 29.71 ppm, corresponding respectively to the olefinic carbons and to the saturated methylene units of the cyclooctadiene ligand. The ^1H NMR spectrum in the same solvent displayed a singlet at 6.10 ppm, with satellites due to coupling with ^{195}Pt, which may be assigned to the four olefinic protons of the cyclooctadiene ligand, and two multiplets at 2.53 and 2.37 ppm, each of them assigned to four saturated protons of the cyclooctadiene ligand. The presence of platinum satellites confirms that the COD ligand remains coordinated to the platinum in solution. The equivalence of the four unsaturated protons also indicates that the coordination of the COD ligand is symmetrical. This cluster **3** has been reported previously,[4] but was obtained in 41% yield only and was not fully characterised by single crystal X-ray diffraction. The molecular structure shown in Fig. 1 (a), in which the metal core adopts an octahedral geometry, was suggested.[4] Nevertheless, an alternative isomer, in which the metal core adopts a monocapped square-based pyramidal geometry, is also possible [Fig. 1 (b)]. Both *closo*-octahedron and monocapped *nido* square-based pyramid are consistent with the PSEPT rules for $[Ru_5PtC(CO)_{14}(COD)]$ **3** (86 electron count). Moreover, Ru_5Pt clusters displaying both structures have been reported in the literature.[4–6] Spectroscopic examination is not expected to distinguish between these two possibilities. Single crystals of **3** were obtained as thin plates by slow diffusion of hexane or ethanol into a dichloromethane solution of the compound, and an X-ray diffraction analysis undertaken. The structure obtained is shown in Fig. 2 and selected bond lengths and angles in Table 1.

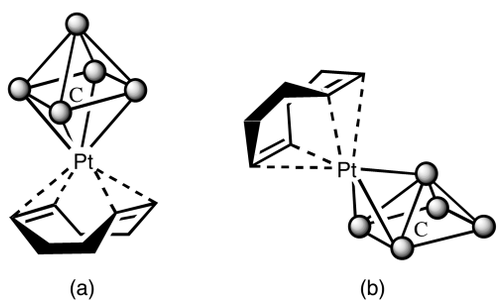

Fig. 1 Possible isomers for $[Ru_5PtC(CO)_{14}(COD)]$ **3**. ○ = Ru. Carbonyls are omitted for clarity.

The asymmetric unit of the structure contains two independent but structurally similar molecules. The Ru_5PtC metal core is octahedral, corresponding to the isomer shown in Fig. 1(a). The Pt(COD) fragment spans the square face of the Ru_5 pyramid, inducing little change in its geometry. The Ru–Ru bonds are slightly longer than those observed in $[Ru_5C(CO)_{15}]$.[7] The values of the Ru(apical)–Ru(basal) bonds range from 2.822(3) to 2.916(3) Å, compared with 2.83(2) Å (mean) in $[Ru_5C$-

Table 1 Selected bond lengths (Å) and angles (°) for $[Ru_5PtC(CO)_{14}(COD)]$ **3**

	Molecule 1	Molecule 2		Molecule 1	Molecule 2
Ru(1)–Pt(1)	3.072(2)	3.074(2)	Pt(1)–C(0)	2.04(2)	2.06(2)
Ru(2)–Pt(1)	2.844(2)	2.858(2)	Ru(1)–Ru(2)	2.937(4)	2.939(4)
Ru(4)–Pt(1)	2.853(2)	2.862(2)	Ru(1)–Ru(4)	2.944(4)	2.967(4)
Ru(5)–Pt(1)	2.962(2)	2.964(2)	Ru(2)–Ru(5)	2.856(4)	2.843(4)
Pt(1)–C(15)	2.22(3)	2.24(3)	Ru(4)–Ru(5)	2.868(4)	2.857(4)
Pt(1)–C(16)	2.30(2)	2.28(3)	Ru(1)–Ru(3)	2.832(3)	2.822(3)
Pt(1)–C(19)	2.21(3)	2.28(3)	Ru(2)–Ru(3)	2.894(3)	2.905(3)
Pt(1)–C(20)	2.25(3)	2.21(3)	Ru(3)–Ru(4)	2.916(3)	2.895(3)
C(15)–C(16)	1.39(3)	1.45(4)	Ru(3)–Ru(5)	2.826(3)	2.835(3)
C(19)–C(20)	1.34(4)	1.40(4)	C–O (mean)	1.169(7)	1.181(12)
Ru(3)–C(0)	2.06(2)	2.05(2)			
Ru(1)–Pt(1)–Ru(2)	59.38(7)	59.27(7)	Ru(4)–Pt(1)–Ru(5)	59.06(8)	58.69(7)
Ru(2)–Pt(1)–Ru(5)	58.89(7)	58.42(7)	Ru(1)–Pt(1)–Ru(4)	59.45(7)	59.86(7)

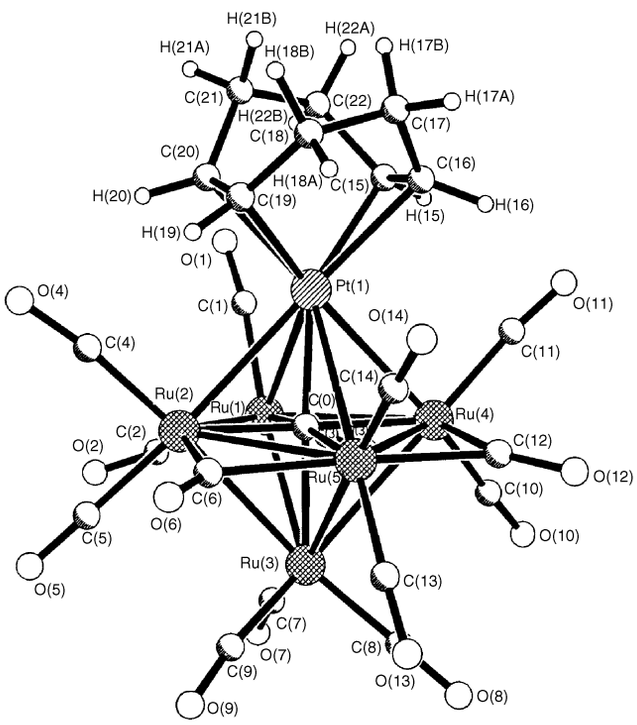

Fig. 2 Molecular structure of $[Ru_5PtC(CO)_{14}(COD)]$ **3**, showing the atom labelling scheme.

$(CO)_{15}]$. It would appear that the coordination of the platinum moiety to the basal ruthenium atoms results in an increase of the Ru(basal)–Ru(basal) bond lengths: these range from 2.843(4) to 2.967(4) Å, compared with 2.86(2) Å (mean) in $[Ru_5C(CO)_{15}]$. The Ru–Pt bonds, varying from 2.844(2) Å to 3.074(2) Å, are within the usual range.[4–6] They are similar to those (≈2.91 Å) observed in the closely related compound $[Ru_5PtC(CO)_{16}]$,[4] and span the upper range of Ru–Pt bond distances listed for compounds characterised by X-ray crystallography. The coordination mode of the cyclooctadiene ligand to the platinum atom remains unchanged, with the C–C bonds involved in the coordination preserving some double bond character. The carbonyl ligands are bent away from the capped side of the molecule, presumably in order to minimise steric repulsion with the unsaturated ring. The Ru(apical)–C(interstitial) bond distance is equivalent [2.06(2) Å in molecule 1; 2.05(2) Å in molecule 2] to that found in $[Ru_5C(CO)_{15}]$ [2.101(18) Å in molecule 1], but the average Ru(apical)–C(0)–Ru(basal) angle is slightly wider. Upon addition of the platinum fragment to the ruthenium cluster, the carbon atom moved towards the plane formed by the four basal ruthenium atoms, to sit nearly perfectly in the middle of the Ru_5Pt octahedron. Two carbonyl ligands bridge Ru–Ru edges [Ru(2)–Ru(5) and Ru(4)–Ru(5) respectively], unlike $[Ru_5C(CO)_{15}]$ where they are all terminal. The Ru–Ru bonds supporting these bridges are consequently shorter than the two other Ru(basal)–Ru(basal) bonds. It is noteworthy that whereas in the past it has been argued that carbonyl bridges are more highly favoured in anionic species as a means of dissipating electron density away from the metal ion, in this work we have observed the opposite effect in the two species **1** and **3**. However, it is relevant that the ligand envelopes in these two species are not the same.

The related reaction of $[PPN]_2[Ru_5C(CO)_{14}]$ **1** with $[Pt(PPh_3)_2Cl_2]$ in dichloromethane at room temperature afforded the bimetallic cluster $[Ru_5PtC(CO)_{14}(PPh_3)_2]$ **4** in 50% yield. The reaction was also performed in the presence of silica, as described above, to release *in situ* the positively charged $[Pt(PPh_3)_2]^{2+}$ fragment. The IR spectrum of **4** displayed peaks attributable to both terminal and bridging carbonyl ligands. Its EI mass spectrum contained the highest mass peak at *m*/*z* 1526 corresponding to $[M - Ph]^+$, followed by peaks attributable to the loss of the phosphine groups and 13 carbonyl ligands. The ^1H NMR spectrum, recorded in CD_2Cl_2, showed only a multiplet at 7.6–7.4 ppm corresponding to the aromatic protons of the PPh_3 groups. The ^{13}C NMR spectrum in CD_2Cl_2 displayed a broad peak at 201.0 ppm due to the CO ligands and a multiplet at 134.2–128.5 ppm corresponding to the C atoms of the phenyl groups. The presence of two phosphine ligands was confirmed by ^{31}P NMR spectroscopy. Thus, the ^{31}P NMR spectrum consisted of a resonance at 29.9 ppm with a ^{195}P–^{31}P coupling of 6280 Hz, assigned to a phosphine ligand bonded directly to a Pt atom. A singlet at 41.8 ppm was also observed and assigned to a phosphine group attached to one of the Ru atoms. Two very weak signals were also displayed at 40.3 ppm and 27.5 ppm (J_{PtP} 6319 Hz) suggesting the presence of another isomer of similar structure. The structural arrangement of the main isomer was confirmed by X-ray structure determination. Suitable crystals were grown overnight from a diethyl ether solution, and the crystal structure of **4** determined by X-ray crystallography. The molecular structure of $[Ru_5PtC(CO)_{14}(PPh_3)_2]$ **4** is shown in Fig. 3 and selected bond parameters are listed in Table 2. As with **3** the Ru_5CPt core is octahedral and as predicted (see above) one phosphine ligand is bound to the platinum atom and the other to an adjacent ruthenium atom. The Pt(1)–Ru(4) bond is bridged by a carbonyl ligand and is significantly shorter than the other Pt–Ru bonds. All the other CO ligands are terminal and bound to the Ru atoms. The Ru–Ru bonds and Ru–Pt bonds are within the usual range and similar to those reported previously for other hexanuclear Ru–Pt mixed-metal clusters.[4,5,8] The interstitial carbon atom is positioned in the centre of the Ru_5Pt octahedron, which is rather typical for this class of compounds. The total electron count for **4** is 86 electrons, which is in line with that predicted for a *closo* octahedral geometry.

The synthesis of the similar compound $[Ru_5PtC(CO)_{14}(PMe_2Ph)_2]$ has been recently reported.[8] Based on the ^{31}P NMR spectrum it was believed to exist in solution as a mixture of

Table 2 Selected bond lengths (Å) and angles (°) for $[Ru_5PtC(CO)_{14}(PPh_3)_2]$ **4**

Ru(2)–Pt(1)	3.0092(6)	Ru(3)–Ru(4)	3.0403(8)
Ru(3)–Pt(1)	2.9599(6)	Ru(4)–Ru(5)	2.9349(9)
Ru(4)–Pt(1)	2.7715(7)	Pt(1)–C(100)	2.062(2)
Ru(5)–Pt(1)	2.9932(6)	Ru(5)–C(100)	2.103(2)
Ru(1)–Ru(2)	2.9256(9)	Pt(1)–P(1)	2.269(2)
Ru(1)–Ru(3)	2.9053(8)	Ru(3)–P(2)	2.377(2)
Ru(1)–Ru(4)	2.8974(9)	Pt(1)–C(11)	2.068(8)
Ru(1)–Ru(5)	2.8247(9)	Ru(4)–C(11)	2.071(8)
Ru(2)–Ru(3)	2.8620(7)	C–O (av.)	1.148(4)
Ru(2)–Ru(5)	2.8342(9)		
Pt(1)–C(100)–Ru(4)	84.94(8)	Ru(1)–C(100)–Ru(5)	85.90(7)
Ru(3)–C(100)–Ru(4)	96.05(8)	Ru(2)–C(100)–Ru(5)	85.69(7)

Table 3 Selected bond lengths (Å) and angles (°) for $[Ru_5PtC(CO)_{15}(PPh_3)]$ **5**

Ru(1)–Pt(1)	2.9004(7)	Pt(1)–C(100)	2.05(1)
Ru(2)–Pt(1)	2.9737(7)	Ru(5)–C(100)	2.08(1)
Ru(3)–Pt(1)	2.7945(8)	Pt(1)–C(9)	2.043(8)
Ru(4)–Pt(1)	3.0817(7)	Ru(3)–C(9)	2.042(8)
Pt(1)–P(1)	2.272(2)	C–O (av.)	1.15(1)
Pt(1)–C(100)–Ru(5)	175.1(5)	Ru(1)–C(100)–Ru(3)	176.7(6)
Ru(2)–C(100)–Ru(4)	171.0(6)		

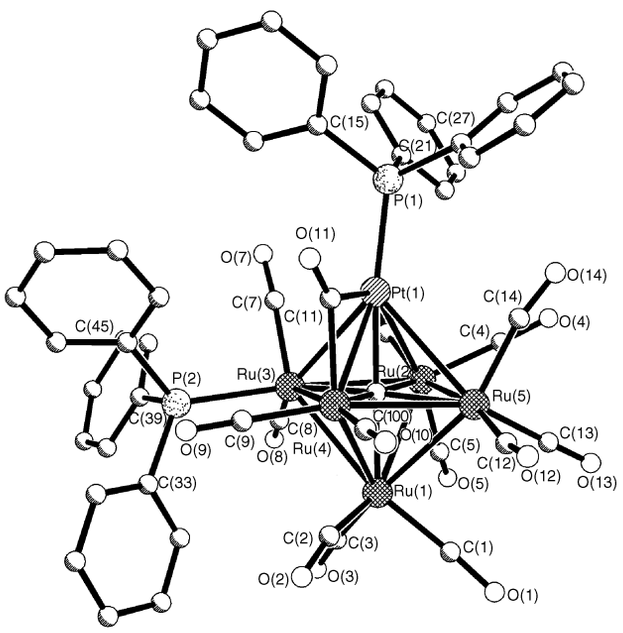

Fig. 3 Molecular structure of $[Ru_5PtC(CO)_{14}(PPh_3)_2]$ **4**, showing the atom labelling scheme.

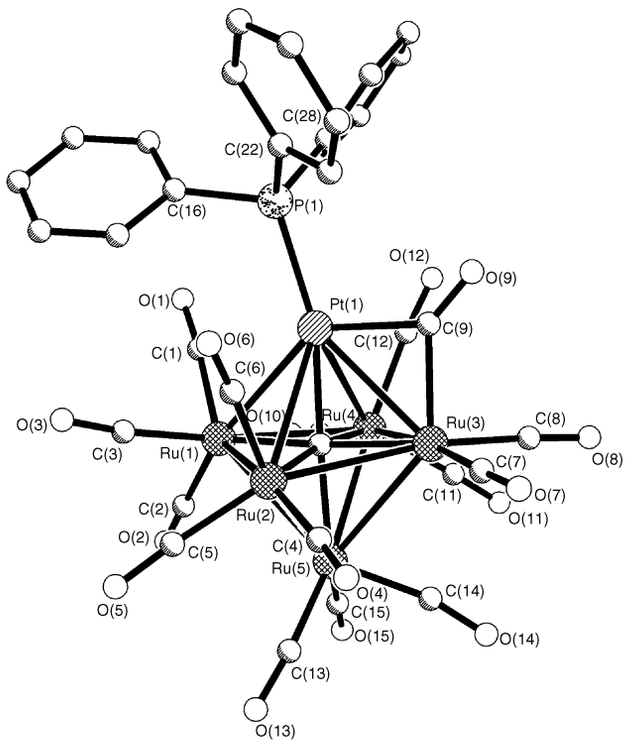

Fig. 4 Molecular structure of $[Ru_5PtC(CO)_{15}(PPh_3)]$ **5**, showing the atom labelling scheme.

three isomers. Even though the isomer with one phosphine ligand on a Ru atom and one on a Pt atom, which we observe in the case of **4**, is the major isomer in solution, $[Ru_5PtC(CO)_{14}(PMe_2Ph)_2]$ crystallises in the form of the isomer that has equivalent phosphine ligands on two opposite basal ruthenium atoms. The ^{31}P NMR spectrum of **4** shows the presence of two isomers in solution at room temperature. When a VT ^{31}P NMR experiment was carried out, the relative intensities of the two resonances of the major isomer changed. As the temperature was raised up to 90 °C, the resonance attributable to the phosphine ligand located on the Ru atom increased in intensity with respect to the resonance corresponding to the phosphine ligand bound to the Pt atom. It may suggest that with an increase of temperature compound **4** also exists in a form of a third isomer which has two equivalent phosphine atoms bound to two opposite basal Ru atoms. Further increase of temperature up to 100 °C resulted in the partial decomposition of compound **4**.

A similar reaction of $[PPN]_2[Ru_5C(CO)_{14}]$ **1** with an excess of $[Pt(CO)(PPh_3)Cl_2]$ at room temperature in dichloromethane in the presence of silica was performed. Apart from the expected product $[Ru_5PtC(CO)_{15}(PPh_3)]$ **5** obtained in 11% yield, the compound $[Ru_5Pt_2C(CO)_{15}(PPh_3)_2]$ **6** was also produced in 16% yield. In the IR spectrum, **5** displayed peaks attributable to both terminal and bridging carbonyl groups. The ESI mass spectrum showed a high intensity peak at *m*/*z* 1426 attributable to $[Ru_5PtC(CO)_{15}(PPh_3)] + MeO^-$ and was followed by a weaker peak at *m*/*z* 1367 corresponding to the loss of $MeCO_2^-$. The spectrum was obtained using a recently developed technique[9,10] based on the formation of a $[M + MeO]^-$ adduct as a result of the treatment of a neutral cluster with NaOMe. The adduct may be easily detected by electrospray ionisation techniques run in the negative mode. The ^1H NMR spectrum in CD_2Cl_2 showed only a multiplet at 7.5–7.4 ppm attributable to 15H of the PPh_3 group and the ^{31}P NMR spectrum showed a singlet at 30.07 ppm with a ^{195}Pt–^{31}P coupling of 6409 Hz, consistent with the view that the phosphine ligand is bound to the Pt atom in solution. Crystals suitable for X-ray structure determination were obtained by slow evaporation of a diethyl ether solution. The molecular structure of **5** is shown in Fig. 4 and selected bond lengths and angles are listed in Table 3. Similar to the compounds described above, **5** contains the central Ru_5CPt octahedron. The phosphine ligand is bound to the platinum atom as indicated by NMR spectroscopy. The Ru–Pt distances lie within the range of 2.9004(7)–3.0817(7) Å and are similar to those reported for $[Ru_5PtC(CO)_{16}]$ [2.777(1)–3.046(1) Å][4] and $[Ru_5PtC(CO)_{15}(PMe_2Ph)]$ [2.773(4)–3.058(4) Å].[8] The Ru–Ru distances range between 2.8146(10)–2.9486(10) Å and are similar to those found in other Ru–Pt mixed-metal clusters.[4–6,8] The previously reported compound $[Ru_5PtC(CO)_{15}(PMe_2Ph)]$ was found to exist as a mixture of two isomers in solution at room temperature.[8] However, this is not the case for **5**. The total electron count of 86 electrons is in line with that predicted for a *closo* octahedral geometry.

The second product isolated from the reaction of **1** with $[Pt(CO)(PPh_3)Cl_2]$ was identified as $[Ru_5Pt_2C(CO)_{15}(PPh_3)_2]$ **6**. Again, the IR spectrum displayed peaks corresponding to both

Table 4 Selected bond lengths (Å) and angles (°) for $[Ru_5Pt_2C(CO)_{15}(PPh_3)_2]$ **6**

Ru(2)–Pt(1)	2.9371(12)	Ru(1)–Pt(2)	2.7604(11)
Ru(3)–Pt(1)	2.9506(12)	Ru(2)–Pt(2)	2.8640(12)
Ru(4)–Pt(1)	2.7695(11)	Ru(3)–Pt(2)	2.8083(12)
Ru(5)–Pt(1)	3.1278(13)	Pt(1)–P(1)	2.266(3)
C–O (av.)	1.15	Pt(2)–P(2)	2.260(4)
Pt(1)–C(0)–Ru(1)	174.0(7)	Ru(1)–Pt(2)–Ru(2)	64.51(3)
Ru(2)–C(0)–Ru(4)	173.7(7)	Ru(2)–Pt(2)–Ru(3)	62.08(4)
Ru(3)–C(0)–Ru(5)	172.5(7)	Ru(3)–Pt(2)–Ru(1)	62.24(3)

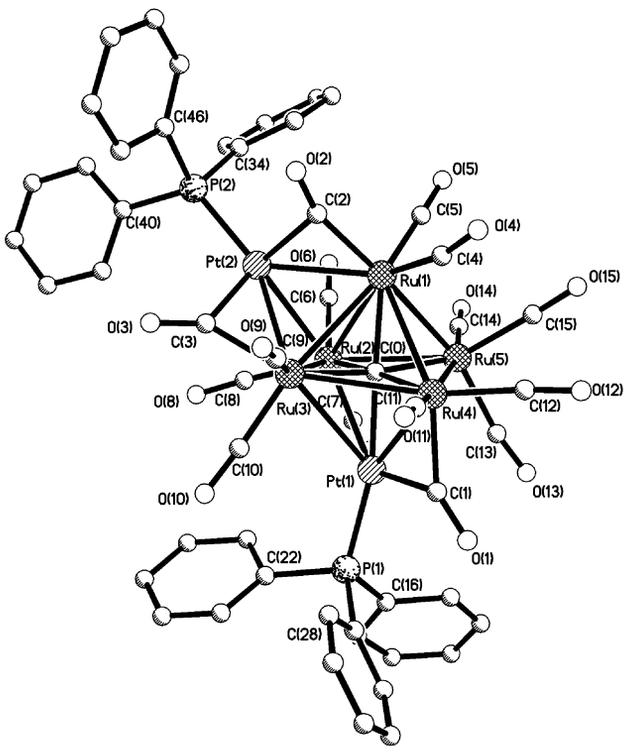

Fig. 5 Molecular structure of $[Ru_5Pt_2C(CO)_{15}(PPh_3)_2]$ **6**, showing the atom labelling scheme.

terminal and bridging carbonyl ligands. The ^1H NMR spectrum in CD_2Cl_2 showed a multiplet at 7.56–7.37 ppm which corresponds to the protons of the phenyl groups. The ^{31}P NMR spectrum displayed two resonances at 77.57 ppm and 31.16 ppm with ^{195}Pt–^{31}P couplings of 6235 Hz and 6391 Hz, respectively, suggesting that both phosphine ligands are bound to the platinum atoms. The absence of $^2J_{PtP}$ coupling suggests that the second Pt atom is capping one of the Ru_3 faces. The peak at 31.16 ppm corresponds to a phosphine ligand bound to the platinum in the axial position of the Ru_5CPt octahedron. The peak at 77.57 ppm is attributed to a phosphine ligand bound to the platinum which is capping one of the faces of the Ru_5PtC octahedron. This structural arrangement was proven by X-ray structure determination. The molecular structure of **6** is shown in Fig. 5 and selected bond parameters are listed in Table 4. A Ru_5Pt octahedron is capped by a second Pt atom at one of its Ru_3-faces. A similar arrangement was found in $[Ru_5Pt_2C(CO)_{13}(COD)_2]$.[4] The Ru–Ru distances are within the expected range of 2.795(2)–3.0030(14) Å and are similar to those reported previously. Though the Ru–Pt distances are also similar in these two compounds, in the case of **6** the distances from Ru to Pt in a capping mode span a somewhat wider range of 2.7695(11)–3.1278(13) Å compared with 2.951(1)–2.829(1) Å found in $[Ru_5Pt_2C(CO)_{13}(COD)_2]$.[4] The total electron count for **6** is 98 electrons which is in line with that predicted for a monocapped octahedral geometry.

In a similar experiment, $[PPN]_2[Ru_6C(CO)_{16}]$ **2** was reacted with $[Pt(COD)Cl_2]$ at room temperature in the presence of

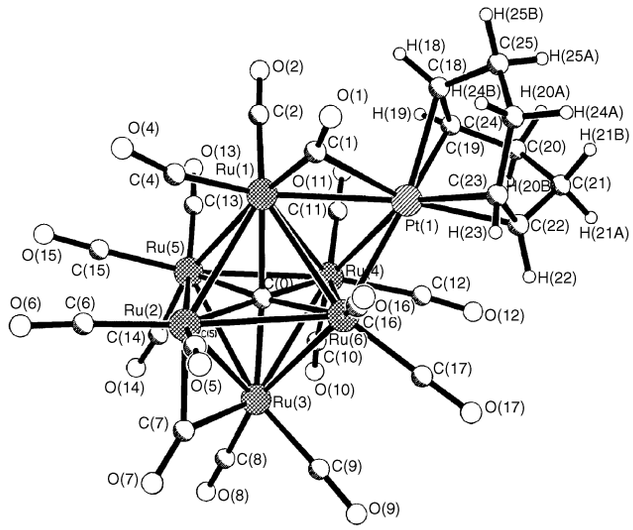

Fig. 6 Molecular structure of $[Ru_6PtC(CO)_{16}(COD)]$ **7**, showing the atom labelling scheme.

silica. Two compounds were isolated by column chromatography: $[Ru_6PtC(CO)_{16}(COD)]$ **7** in 70% yield and $[Ru_6Pt_2C(CO)_{15}(COD)_2]$ **8** in less than 1% yield. Again the main product is the expected species, arising from the addition of a "Pt(COD)" fragment to the starting Ru_6 cluster. The syntheses of two analogous compounds $[Ru_nPtC(CO)_m(COD)]$ ($n = 5$, $m = 14$ and $n = 6$, $m = 16$) in high yield following similar preparation routes, starting from $[Ru_nC(CO)_m]^{2-}$ and $[Pt(COD)Cl_2]$, demonstrates the effectiveness of the use of a chloride scavenger to produce fragments with controlled reactivity.

The infrared spectrum of $[Ru_6PtC(CO)_{16}(COD)]$ **7** in CH_2Cl_2 displays CO stretching bands attributable to both terminal and bridging carbonyls. When analysed by mass spectrometry, the only peaks observed are those corresponding to the formulation $[Ru_6C(CO)_{17}]$: degradation of $[Ru_6PtC(CO)_{16}(COD)]$ **7** to some $[Ru_6C(CO)_{17}]$ must occur in the spectrometer. The ^{13}C NMR spectrum displays peaks at 97.50 ppm assigned to unsaturated CH of the COD ligand, and at 29.71 ppm assigned to CH_2, along with a singlet at 200.94 ppm, assigned to the carbonyl ligands. Only one signal is observed due to rapid exchange processes between all the carbonyls, averaging their chemical environments. The ^1H NMR spectrum contains two multiplets at 2.60 and 2.18 ppm assigned to eight saturated protons and a singlet at 5.73 ppm with platinum satellites assigned to the four unsaturated protons of the COD ligand. This indicates that the integrity of the Pt(COD) fragment is kept in solution. The molecular structure of **7** was determined by X-ray diffraction analysis and is presented in Fig. 6. Selected bond lengths and angles are presented in Table 5.

The molecular structure consists of an intact $Ru_6C(CO)_{16}$ unit, with one triangular face of the Ru_6 octahedron capped by the Pt(COD) fragment. All bond distances and bond angles of the Ru_6 octahedron remain almost unchanged. Thus, the Ru–Ru bonds range between 2.7776(14) and 2.9790(14) Å, which is very similar to the values 2.827(5)–3.034(5) Å found in $[Ru_6C(CO)_{17}]$[11] and the Ru–Ru bonds spanned by the platinum atom are not particularly changed with respect to the unsubstituted cluster. The Ru–Pt bond distances, varying from 2.6097(12) Å to 2.9283(12) Å, are within the normal range. Values ranging from 2.627(1) to 2.857(1) Å are found where the Pt(COD) fragment caps a Ru_3 triangular face in $[Ru_5Pt_2C(CO)_{13}(COD)_2]$.[4] The conformation of the cyclooctadiene ligand is very similar to what was observed in $[Ru_5PtC(CO)_{14}(COD)]$ **3**. The C–C bonds coordinated to the platinum are only slightly longer than a typical C=C double bond [1.378(17) Å and 1.382(15) Å]. Fifteen carbonyl ligands are terminally bound, and one is bridging a Ru–Ru bond, which is consequently the shortest [Ru(2)–Ru(3) = 2.7776(14) Å]. The

Table 5 Selected bond lengths (Å) and angles (°) for $[Ru_6PtC(CO)_{16}(COD)]$ **7**

Ru(1)–Pt(1)	2.7866(11)	Ru(1)–Ru(6)	2.8388(16)
Ru(4)–Pt(1)	2.9283(12)	Ru(2)–Ru(6)	2.9714(14)
Ru(6)–Pt(1)	2.6097(12)	Ru(3)–Ru(6)	2.9485(14)
Pt(1)–C(18)	2.264(10)	Ru(4)–Ru(6)	2.8597(14)
Pt(1)–C(19)	2.237(10)	Ru(1)–Ru(2)	2.9700(14)
Pt(1)–C(22)	2.188(10)	Ru(2)–Ru(3)	2.7776(14)
Pt(1)–C(23)	2.177(10)	Ru(3)–Ru(4)	2.9790(14)
Ru(1)–Ru(5)	2.8530(14)	Ru(4)–Ru(1)	2.9454(14)
Ru(2)–Ru(5)	2.9232(15)	C(18)–C(19)	1.378(17)
Ru(3)–Ru(5)	2.9631(16)	C(22)–C(23)	1.382(15)
Ru(4)–Ru(5)	2.8479(13)	C–O (mean)	1.142(4)
Ru(1)–Pt(1)–Ru(4)	61.99(3)	Ru(4)–Pt(1)–Ru(6)	61.86(3)
Ru(1)–Pt(1)–Ru(6)	63.38(4)		

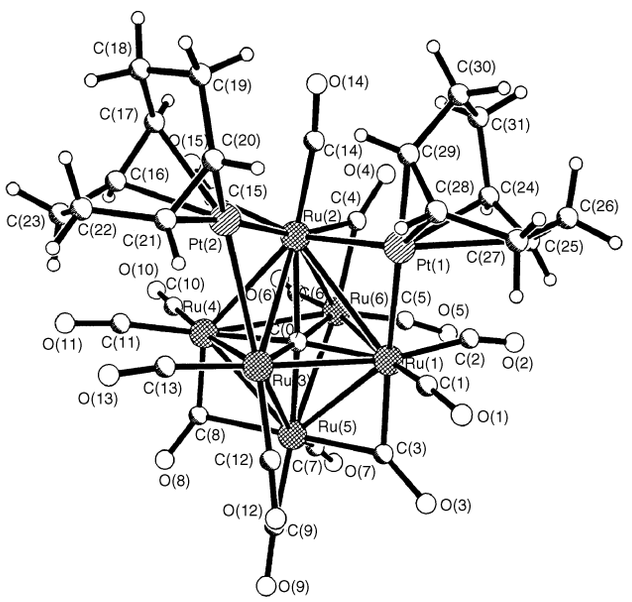

Fig. 7 Molecular structure of $[Ru_6Pt_2C(CO)_{15}(COD)_2]$ **8**, showing the atom labelling scheme.

monocapped octahedral geometry of the cluster core is in line with its 98 electron count.

The compound $[Ru_6Pt_2C(CO)_{15}(COD)_2]$ **8** was also obtained as a by-product but in very low yield. Its infrared spectrum displays CO stretching bands attributable to terminal and bridging carbonyl ligands. Small crystals of **8** were obtained from a dichloromethane solution layered with hexane, and the molecular structure was determined by single crystal X-ray diffraction. The asymmetric unit of the crystal structure contains two independent but structurally similar molecules. The molecular structure obtained is shown in Fig. 7 and selected bond lengths and angles in Table 6.

Essentially, it consists of an octahedron of six ruthenium atoms, linked to two Pt(COD) units. The analogous cluster $[Os_6Pt_2(CO)_{17}(COD)_2]$ has been reported to display an octahedron of osmium atoms with two opposite faces Pt-capped.[12] Surprisingly, the Pt(COD) moieties in **8** do not cap Ru_3 triangular faces but bridge Ru–Ru edges. Moreover, the second Pt(COD) fragment is not on the opposite side of the octahedron. Rather, it is bridging a Ru–Ru bond that belongs to the same Ru_3 triangle as the edge bridged by the first platinum. Disorder associated with the Ru_6 octahedron did not allow a precise location of the carbonyl ligands. However, the geometry of the Ru_6 carbide octahedron remained mostly unchanged, with Ru–Ru, Ru–C and C–O bond lengths in the expected range. The Ru–Ru bonds bridged by the platinum atoms are considerably longer than the other Ru–Ru bond distances: 3.120(5) Å for Ru(2)–Ru(1) and 3.020(4) Å for Ru(2)–Ru(3) in molecule 1; 3.114(5) Å for Ru(2)–Ru(1) and 3.039(5) Å for Ru(2)–Ru(3) in molecule 2. The Ru–Pt bonds are within the normal range, varying from 2.751(4) Å to 2.996(4) Å, to be compared with 2.844(2)–3.074(2) Å observed in the case of $[Ru_5PtC(CO)_{14}(COD)]$ **3**, and 2.6097(12)–2.9283(12) Å in $[Ru_6PtC(CO)_{16}(COD)]$ **7**. They are slightly longer than the commonest Ru–Pt bond length reported in the literature. The two cyclooctadiene ligands are coordinated to the platinum atoms in a similar fashion to that observed in the mono-adducts, with little change from the geometry of the starting $[Pt(COD)Cl_2]$. The COD ligand bound to Pt(1) is slightly asymmetrically coordinated, *i.e.* the Pt–C(olefinic) bond lengths vary from 2.07(4) to 2.52(4) Å in molecule 1. Each ruthenium atom bears two terminal carbonyl ligands, and three Ru–Ru bonds are spanned by bridging CO's, inducing a shortening in their distances [Ru(5)–Ru(4): 2.766(5) Å, Ru(5)–Ru(1): 2.831(5) Å and Ru(6)–Ru(2): 2.792(5) Å in molecule 1]. The 110 electron count for $[Ru_6Pt_2C(CO)_{15}(COD)_2]$ **8** is consistent with a central octahedral core. Using the condensed polyhedra approach, the structure obtained corresponds to an electron count of 114. This is in line with previous reports on platinum-containing clusters that do not obey the normal electron counting rules and appear to be electron deficient.[13] It is of interest to note that the explanation for this deficiency has often been linked to the ability of platinum to be a 16 electron metal centre. For clusters **3**–**7**, the platinum component has been assigned an 18 electron count, the normal electron counting rules were always obeyed, and the platinum fragments were capping faces. However, in the case of **8**, the Pt moieties are bridging edges, which might be related to a (more) planar coordination geometry associated with a 16 electron count. We wish to point out nevertheless that attributing a precise electron count to each individual metal atom in cluster compounds is not really appropriate.

In an attempt to obtain **8** in higher yield, **2** was reacted with two equivalents of $[Pt(COD)Cl_2]$ in the presence of silica. A solution of **2** was added dropwise to a solution of $[Pt(COD)Cl_2]$ in order to favour the addition of several "Pt(COD)" fragments to the Ru_6 cluster. Nevertheless, the one-to-one adduct $[Ru_6PtC(CO)_{16}(COD)]$ **7** was still the main product of the reaction. This suggests that **7** is a thermodynamic sink, driving the reaction towards its formation under any experimental conditions. The compound **7** was also reacted further with $[Pt(COD)Cl_2]$ in dichloromethane in the presence of silica. No reaction was observed to occur, even after heating under reflux for 24 hours. This, on the other hand, suggests that the mechanism of formation of **8** does not involve stepwise addition of monometallic platinum fragments to the ruthenium cluster, with $[Ru_6PtC(CO)_{16}(COD)]$ **7** as an intermediate. Rather, it would seem to involve either a concerted addition or formation of a Pt dimer prior to addition to the Ru_6 cluster. This latter possibility would account for the low yield and the fact that the two Pt(COD) fragments are bound to the same side of the molecule.

Experimental

All the reactions were carried out using standard Schlenk techniques, under water- and oxygen-free nitrogen. All solvents were dried and distilled immediately before use. Reactants and chemicals were purchased from Aldrich Chemicals and used without further purification. The silica used in reaction media and for column chromatography was silica gel 60 (0.040–0.063 mm) purchased from Merck. The clusters $[Ru_6C(CO)_{17}]$[14] and $[Ru_5C(CO)_{15}]$[7,15] were synthesised following literature procedures.

All chromatographic separations were performed on the open bench without any precaution to exclude air. Thin-layer chromatography (TLC) was carried out using glass plates (20 × 20 cm) coated with a layer of silica gel 60 F_{254}, supplied by Merck. Column chromatography was carried out using a 40 cm long glass column with an internal diameter of 3 cm and 50 ml

Table 6 Selected bond lengths (Å) and angles (°) for $[Ru_6Pt_2C(CO)_{15}(COD)_2]$ **8**

	Molecule 1	Molecule 2		Molecule 1	Molecule 2
Ru(1)–Pt(1)	2.814(4)	2.798(4)	C(28)–C(29)	1.35(3)	1.35(2)
Ru(2)–Pt(1)	2.936(4)	2.975(4)	Ru(2)–Ru(4)	2.952(5)	2.968(5)
Ru(2)–Pt(2)	2.769(4)	2.751(4)	Ru(3)–Ru(4)	2.885(5)	2.930(5)
Ru(3)–Pt(2)	2.996(4)	2.990(4)	Ru(5)–Ru(4)	2.766(5)	2.780(5)
Pt(1)–C(24)	2.26(4)	2.18(4)	Ru(6)–Ru(4)	2.982(5)	2.984(5)
Pt(1)–C(25)	2.52(4)	2.23(4)	Ru(2)–Ru(1)	3.120(5)	3.114(5)
Pt(1)–C(28)	2.09(4)	2.42(4)	Ru(3)–Ru(1)	2.822(5)	2.825(5)
Pt(1)–C(29)	2.07(4)	2.31(4)	Ru(5)–Ru(1)	2.831(5)	2.873(5)
Pt(2)–C(16)	2.34(4)	2.08(4)	Ru(6)–Ru(1)	2.882(5)	2.878(5)
Pt(2)–C(17)	2.38(4)	2.15(4)	Ru(2)–Ru(3)	3.020(4)	3.039(5)
Pt(2)–C(20)	2.22(4)	2.30(4)	Ru(3)–Ru(5)	2.929(5)	2.953(5)
Pt(2)–C(21)	2.16(4)	2.16(4)	Ru(5)–Ru(6)	2.935(5)	2.935(5)
C(16)–C(17)	1.35(3)	1.36(3)	Ru(6)–Ru(2)	2.792(5)	2.761(5)
C(20)–C(21)	1.36(3)	1.35(3)	C–O (mean)	1.17(2)	1.20(2)
C(24)–C(25)	1.34(3)	1.36(3)			
Ru(1)–Pt(1)–Ru(2)	65.70(10)	65.20(11)	Ru(2)–Pt(2)–Ru(3)	63.03(10)	63.78(10)

reservoir, packed with silica gel 60 (0.040–0.063 mm), also purchased from Merck. The eluents used for both column and thin-layer chromatography were standard grade laboratory solvents.

Infrared spectra were collected in dichloromethane solution unless otherwise stated, using a NaCl liquid cell (0.5 mm path length) supplied by Specac Ltd., on a Perkin-Elmer Paragon 1000 FT-IR spectrometer. The mass spectra were obtained on a Kratos Concept spectrometer and on a Kratos MS890 spectrometer, using electron impact ionisation (EI) in positive mode or on a Micromass Quattro-LC spectrometer using electrospray ionisation technique (ESI) in negative mode. The ^{13}C and ^{1}H NMR spectra were recorded on a Bruker AM-400 or DPX-400 instrument, while ^{31}P NMR spectra were recorded on Bruker AC-250 or DPX-400 instruments. The elemental analyses were made by the microanalysis service of the department.

Crystallography

Single crystal X-ray diffraction analyses were performed by the crystallography service of the department on one of three instruments, equipped with devices for low-temperature data collection: a Rigaku AFC-7R or RAXIS-11 four-circle diffractometer with a rotating-anode Mo-Kα source, or a Nonius Kappa CCD system with a sealed-tube Mo-Kα source. The structures were solved by direct methods using the TEXSAN[16] or SHELXS-97[17] programs, and refined by full-matrix least-squares on F^2 with SHELXL-93[18] or SHELXL-97[17] software packages. All non-hydrogen atoms in compounds **4**, **5** and **7**, apart from those for the solvent molecules and disordered groups, were refined with anisotropic atomic displacement parameters. In the case of **3**, **6** and **8** only Ru, Pt and P atoms were refined with anisotropic atomic displacement parameters. All hydrogen atoms were placed in idealised positions, assigned isotropic displacement parameters and allowed to ride on the parent carbons. The crystal data for **3**–**8** is summarised in Table 7.

CCDC reference numbers 168615–168620.

See http://www.rsc.org/suppdata/dt/b1/b105844b/ for crystallographic data in CIF or other electronic format.

Syntheses

Preparation of $[PPN]_2[Ru_5C(CO)_{14}]$ 1. In a typical experiment, 110 mg of $[Ru_5C(CO)_{15}]$ (0.117 mmol) were suspended in methanol (20 ml). Two pellets of KOH were added and the mixture stirred at room temperature for half an hour. Bis(triphenylphosphine)iminium chloride (PPNCl) was added (135 mg, 0.235 mmol), provoking precipitation. The red microcrystalline solid was collected by filtration and washed three times with hexane. Yield: 94%. ν_{max}/cm^{-1} (CO) 2031w, 1974vs, 1962s(sh), 1915m, 1747w(br). This reaction could be scaled up to 743 mg of starting material.

Preparation of $[PPN]_2[Ru_6C(CO)_{16}]$ 2. $[Ru_6C(CO)_{17}]$ (100 mg, 0.0913 mmol) was suspended in methanol (20 ml). Two pellets of KOH were added, and the mixture stirred at room temperature for half an hour. PPNCl (100 mg, 0.174 mmol) was added to the deep red solution, and a bright orange precipitate was collected by filtration, washed with hexane, and dried *in vacuo*. Yield: 94%. ν_{max}/cm^{-1} (CO) 1976vs, 1917w, 1782w. The reaction could be successfully scaled up to 1 g of starting material, and the anion $[Ru_6C(CO)_{16}]^{2-}$ could also be isolated as its $[Ph_4As]^+$, $[Et_4N]^+$ or $[Ph_4P]^+$ salt.

Preparation of $[Ru_5PtC(CO)_{14}(COD)]$ 3. $[PPN]_2[Ru_5C(CO)_{14}]$ **1** (500 mg, 0.2517 mmol) was dissolved in dichloromethane (130 ml). One molar equivalent (94 mg) of $[Pt(COD)Cl_2]$ and 10 spatulas of silica were added, inducing an immediate darkening of colour. After stirring at room temperature for 4 hours, the mixture was filtered and evaporated on a rotary evaporator. The crude product was then purified by thin-layer chromatography, using hexane–dichloromethane (7 : 3, v/v) as eluent, leading to isolation of one main red–orange microcrystalline compound: $[Ru_5PtC(CO)_{14}(COD)]$ **3**. Yield: 256 mg (84%). The compound was soluble in dichloromethane, acetone, THF and toluene, and insoluble in hexane and water. Found: C, 22.82; H, 1.06%. $C_{23}H_{12}O_{14}Pt_1Ru_5$ requires C, 22.78; H, 1.00%. IR(CH_2Cl_2): ν_{max}/cm^{-1} (CO) 2077m, 2049s, 2033s, 2011s, 1989w(sh), 1965w(sh), 1818w. IR(Nujol mull): ν_{max}/cm^{-1} (CO) 2069m, 2035s, 2011s, 1992s, 1950w(sh), 1824w. ^{1}H NMR ($CDCl_3$) δ: 6.10 (s + d, 4H, $^{2}J_{PtH}$ 74.46 Hz), 2.53 (m, 4H, br), 2.37 (m, 4H, br). ^{13}C NMR ($CDCl_3$) δ: 87.37 (CH), 29.71 (CH_2). EI-MS: *m*/*z*: 1214 [calc. for $Ru_5C(CO)_{14}Pt(COD)$: 1213, M^+], with the loss of the COD ligand, followed by loss of 14 CO ligands observed. Crystals suitable for X-ray crystallographic analysis were obtained overnight by slow diffusion of hexane or ethanol into a dichloromethane solution of **3**.

Preparation of $[Ru_5PtC(CO)_{14}(PPh_3)_2]$ 4. To a solution of $[PPN]_2[Ru_5C(CO)_{14}]$ **1** (100 mg, 0.05 mmol) in CH_2Cl_2 (20 ml) one equivalent of $[Pt(PPh_3)_2Cl_2]$ (40 mg, 0.05 mmol) and two spatulas of silica were added. The mixture was stirred for 4 hours at room temperature. Subsequently, the silica was filtered off and the solvent evaporated to dryness *in vacuo*. The resulting product was dissolved in the minimum amount of CH_2Cl_2 and the mixture separated by TLC [dichloromethane–hexane (2 : 3, v/v) as eluent]. The dark-red band was identified as **4**. Yield: 40 mg (0.025 mmol, 50%). Found: C, 38.12; H, 2.09; P, 3.67. $C_{51}H_{30}O_{14}P_2PtRu_5$ requires C, 37.60; H, 1.86; P, 3.80%; ν_{max}/cm^{-1} (CO) 2069m, 2031s, 2022vs, 1994m(sh), 1975w,

1945w and 1816m(br); ^{1}H NMR (300 K, CD_2Cl_2) δ: 7.6–7.4 [m, 30H, $P(C_6H_5)_3$]; ^{31}P NMR (300 K, CD_2Cl_2) δ(major isomer): 41.8 [s, $P(C_6H_5)_3$], 29.9 [s, $P(C_6H_5)_3$, $^1J_{PtP}$ 6280 Hz]; δ(minor isomer): 40.3 [d, $P(C_6H_5)_3$], 27.5 [d, $P(C_6H_5)_3$, $^1J_{PtP}$ 6319 Hz]; ^{13}C NMR (300 K, CD_2Cl_2) δ: 201.0 (m, CO), 134.2–128.5 (m, C_6H_5); EI-MS: *m*/*z* 1526 {calc. for $Ru_5PtC(CO)_{13}(PPh_3)(PPh_2)$: 1526, $[M - Ph]^+$}. Crystals suitable for X-ray determination were grown by slow evaporation of a diethyl ether solution of **4**.

Preparation of $[Ru_5PtC(CO)_{15}(PPh_3)]$ 5 and $[Ru_5Pt_2C(CO)_{15}(PPh_3)_2]$ 6. To a solution of $[PPN]_2[Ru_5C(CO)_{14}]$ **1** (100 mg, 0.05 mmol) in CH_2Cl_2 (20 ml) an excess of $[Pt(CO)(PPh_3)Cl_2]$ (61 mg, 0.11 mmol) and two spatulas of silica were added. The mixture was stirred for 30 minutes at room temperature. In the following step, the silica was filtered off and the solvent evaporated to dryness *in vacuo*. The crude product was dissolved in a minimum amount of CH_2Cl_2 and purified by TLC [dichloromethane–hexane (2 : 3, v/v) as eluent]. The top red band was identified as **5** [Yield: 10 mg (0.007 mmol, 11%)], and the second brown band was identified as **6** [Yield: 20 mg (0.011 mmol, 16%)].

Analysis for **5**: Found: C, 29.16; H, 1.26; P, 2.08. $C_{34}H_{15}O_{15}PPtRu_5$ requires C, 29.28; H, 1.08; P, 2.22%; ν_{max}/cm^{-1} (CO) 2086m, 2057s, 2037vs, 1994,m and 1833m(br); ^{1}H NMR (300 K, CD_2Cl_2) δ: 7.47–7.41 [m, 15H, $P(C_6H_5)_3$]; ^{31}P NMR (300 K, CD_2Cl_2) δ: 30.07 [s, $P(C_6H_5)_3$, $^1J_{PtP}$ 6409 Hz]; ESI-MS *m*/*z* 1426 $[M + MeO]^-$. Crystals suitable for X-ray determination were grown by slow evaporation of a diethyl ether solution and by layering a CH_2Cl_2 solution with hexane.

Analysis for **6**: Found: C, 33.16; H, 2.21; P, 3.15. $C_{52}H_{30}O_{15}P_2Pt_2Ru_5$ requires C, 33.72; H, 1.63; P, 3.34%; ν_{max}/cm^{-1} (CO) 2071m, 2035s, 2016m, 1982m and 1824m(br); ^{1}H NMR (300 K, CD_2Cl_2) δ: 7.56–7.37 [m, 30H, $P(C_6H_5)_3$]; ^{31}P NMR (300 K, CD_2Cl_2) δ: 77.57 [s, $P(C_6H_5)_3$, $^1J_{PtP}$ 6235 Hz], 31.16 [t, $P(C_6H_5)_3$, $^1J_{PtP}$ 6391 Hz]. Crystals suitable for X-ray determination were grown by slow evaporation of a toluene–hexane solution.

Preparation of $[Ru_6PtC(CO)_{16}(COD)]$ 7 and $[Ru_6Pt_2C(CO)_{15}(COD)_2]$ 8. $[PPN]_2[Ru_6C(CO)_{16}]$ **2** (200 mg, 0.0933 mmol) was dissolved in 45 ml dichloromethane. A slight excess (40 mg) of $[Pt(COD)Cl_2]$ and two spatulas of silica were added, and the mixture stirred for three days at room temperature. The silica was removed by filtration and the filtrate evaporated to dryness. The crude product was purified by column chromatography, using hexane–dichloromethane (3 : 2, v/v) as eluent, which led to the isolation of a main dark orange fraction, $[Ru_6PtC(CO)_{16}(COD)]$ **7**, in 70% yield (90 mg) and a minor orange fraction, $[Ru_6Pt_2C(CO)_{15}(COD)_2]$ **8**, in very low yield (0.6 mg, < 1%).

Analysis for **7**: Found: C, 24.51; H, 1.76%. $C_{25.50}H_{13}ClO_{16}Pt_1Ru_6$ requires C, 21.68; H, 0.92%; ν_{max}/cm^{-1} (CO) 2077m, 2034s, 1999m, 1976w(sh), 1947w(sh), 1822w. ^{1}H NMR ($CDCl_3$) δ: 5.73 (s + d, 4H, $^2J_{PtH}$ = 65 Hz), 2.60 (m, 4H, br), 2.18 (m, 4H, br). ^{13}C NMR ($CDCl_3$) δ: 200.94 (C), 97.50 (CH), 29.71 (CH_2). EI-MS: *m*/*z*: 1094 [calc. for $Ru_6C(CO)_{17}$: 1095], with the loss of 17 CO ligands observed. Crystals suitable for X-ray diffraction structure determination were grown by slow diffusion of either hexane or ethanol into a solution of **7** in dichloromethane.

Analysis for **8**: ν_{max}/cm^{-1} (CO) 2057m, 2026m, 2011s, 1970w(br), 1857w(br), 1823w(br). Very small crystals were obtained by slow diffusion of hexane into a dichloromethane solution of **8**.

The same reaction was carried out in a 1 : 2 ratio in the following way: $[Pt(COD)Cl_2]$ (35 mg. 0.0932 mmol) was dissolved in dichloromethane (15 ml). Two spatulas of silica were added. A solution of $[PPN]_2[Ru_6C(CO)_{16}]$ **2** (100 mg, 0.0466 mmol) in 15 ml dichloromethane was added dropwise, and the mixture stirred at room temperature overnight. Monitoring by IR spectroscopy showed that the expected

Table 7 Crystal data for compounds **3**–**8**

	3	**4**	**5**	**6**	**7**	**8**
Chemical formula	$C_{23}H_{12}O_{14}PtRu_5$	$C_{59}H_{50}O_{16}P_2PtRu_5$	$C_{34}H_{15}O_{15}PPtRu_5$	$C_{52}H_{30}O_{15}P_2Pt_2Ru_5$	$C_{25.50}H_{13}ClO_{16}PtRu_6$	$C_{32}H_{24}O_{15}Pt_2Ru_6$
M	1212.77	1777.37	1394.87	1852.23	1412.32	1645.11
Crystal system	Tetragonal	Monoclinic	Monoclinic	Monoclinic	Monoclinic	Monoclinic
Space group	$P4_12_12$	$P2_1/c$	$P2_1$	$P2_1/n$	$P2_1/c$	$P2_1/c$
a/Å	17.302(4)	17.4020(3)	9.2740(3)	10.0384(4)	16.368(7)	12.983(5)
b/Å	17.302(4)	13.7880(4)	23.5940(8)	53.540(2)	12.623(5)	35.475(8)
c/Å	38.128(5)	26.6030(7)	9.8430(2)	10.4442(4)	17.370(5)	18.366(7)
β/°		106.769(2)	116.489(2)	109.278(1)	112.79(2)	92.63(4)
V/Å^3	11414(4)	6111.7(3)	1927.7(1)	5298.5(4)	3309(2)	8450(5)
Z	16	4	2	4	4	8
μ(Mo-Kα)/mm^{-1}	7.531	3.603	5.634	6.773	7.029	8.740
No. of reflections collected	11235	19005	13788	10716	7824	19995
No. of independent reflections	5768	10689	6400	6730	7568	13344
R_{int}	0.0370	0.0428	0.0491	0.0534	0.0461	0.1080
Final *R* indices [$I > 2\sigma(I)$] *R1*, *wR2*	0.0433, 0.0937	0.0432, 0.0981	0.0333, 0.0801	0.0600, 0.1789	0.0494, 0.1036	0.1129, 0.2343
(all data)	0.0768, 0.1101	0.0715, 0.1081	0.0365, 0.0819	0.0726, 0.1968	0.0798, 0.1160	0.2329, 0.2882

$[Ru_6Pt_2C(CO)_{15}(COD)_2]$ **8** was not obtained. Upon addition of more $[Pt(COD)Cl_2]$ and heating under reflux for two days, $[Ru_6PtC(CO)_{16}(COD)]$ **7** was obtained as the main product. ν_{max}/cm^{-1} (CO) 2077m, 2034s, 1998m, 1976w(sh), 1947w(sh), 1820w.

Attempt to obtain $[Ru_6Pt_2C(CO)_{15}(COD)_2]$ 8 from $[Ru_6PtC(CO)_{16}(COD)]$ 7. $[Ru_6PtC(CO)_{16}(COD)]$ **7** (57 mg, 0.0418 mmol) was dissolved in dichloromethane (20 ml). One molar equivalent of $[Pt(COD)Cl_2]$ (16 mg) and two spatulas of silica were added, and the solution stirred at room temperature for two days, during which no changes in the infrared spectra could be observed. The mixture was then heated under reflux for 24 hours, inducing no changes in the IR spectra either. The heating was then discontinued.

Acknowledgements

We are grateful to Dr John E. Davies for data collection and structure refinement for compounds **3**, **7** and **8** and to the European Commission and Newnham College, Cambridge, for funding to S. H., to the Cambridge Overseas Trust (Schlumberger Research) and ICI for funding to T. K., and to ICI and the EPSRC for a grant to B. F. G. J.

References

1 R. Raja, G. Sankar, S. Hermans, D. S. Shephard, S. Bromley, J. M. Thomas, B. F. G. Johnson and T. Maschmeyer, *Chem. Commun.*, 1999, 1571.
2 S. Hermans, R. Raja, J. M. Thomas, B. F. G. Johnson, G. Sankar and D. Gleeson, *Angew. Chem., Int. Ed.*, 2001, **40**, 1211.
3 D. S. Shephard, T. Maschmeyer, G. Sankar, J. M. Thomas, D. Ozkaya, B. F. G. Johnson, R. Raja, R. D. Oldroyd and R. G. Bell, *Chem. Eur. J.*, 1998, **4**, 1214.
4 R. D. Adams and W. Wu, *J. Cluster Sci.*, 1991, **2**, 271.
5 R. D. Adams and W. Wu, *J. Cluster Sci.*, 1993, **4**, 245.
6 R. D. Adams and W. Wu, *Organometallics*, 1993, **12**, 1238.
7 B. F. G. Johnson, J. Lewis, J. N. Nicholls, J. Puga, P. R. Raithby, M. J. Rosales, M. McPartlin and W. Clegg, *J. Chem. Soc., Dalton Trans.*, 1983, 277.
8 R. D. Adams, B. Captain, W. Fu and P. J. Pellechia, *Chem. Commun.*, 2000, 937.
9 W. Henderson, J. S. McIndoe, B. K. Nicholson and P. J. Dyson, *Chem. Commun.*, 1996, 1183.
10 W. Henderson, J. S. McIndoe, B. K. Nicholson and P. J. Dyson, *J. Chem. Soc., Dalton Trans.*, 1998, 519.
11 A. Sirigu, M. Bianchi and E. Benedetti, *Chem. Commun.*, 1969, 596.
12 C. Couture and D. H. Farrar, *J. Chem. Soc., Dalton Trans.*, 1986, 1395.
13 L. J. Farrugia, *Adv. Organomet. Chem.*, 1990, **31**, 301.
14 C. R. Eady, B. F. G. Johnson and J. Lewis, *J. Chem. Soc., Dalton Trans.*, 1975, 2606.
15 D. H. Farrar, P. F. Jackson, B. F. G. Johnson, J. Lewis and J. N. Nicholls, *J. Chem. Soc., Chem. Commun.*, 1981, 415.
16 TEXSAN, version 1.7, Molecular Structure Corporation, Houston, TX, 1995.
17 G. M. Sheldrick, SHELX-97, University of Göttingen, 1997.
18 G. M. Sheldrick, SHELXL-93, University of Göttingen, 1993.